# Line Detection in Strongly Noise-Corrupted Images

Dietmar Kunz and Bernhard Schweiger

Institut für Medien- und Phototechnik
Fachhochschule Köln, Betzdorfer Str. 2, 50679 Köln
Email: dietmar.kunz@fh-koeln.de

**Abstract.** A novel method for detection of thin lines in strongly noise-corrupted images is presented. The method can be applied e.g. for guide wire detection in X-ray fluoroscopy sequences. In a first step, the responses of a set of angular separable filters are calculated and the maximum of the filter responses is taken. Application of a subsampling scheme allows to reduce the computational effort. In a second step, a flood filling algorithm is used to eliminate worm-like artifacts arising from random line structures in the noise. Depending on the line curvature, signal-to-noise ratio (SNR) improvements of 27 dB have been achieved.

## 1 Introduction

Detecting thin lines in strongly noise-corrupted images represents a very difficult task in image processing. In medical image processing, this problem arises for example in noise reduction and contrast enhancement of X-ray fluoroscopy sequences. In particular, guide wires have to be made or maintained visible to support the examining physician in cardio-vascular catheter interventions. This implies that such guide wires can be distinguished from surrounding tissue despite of their small area and poor contrast.

For a particular point being recognized as part of a thin line, it has to differ significantly from its environment after appropriate filtering. Significant differences, however, can only be expected if the applied filter kernel is optimally matched to the – unknown – orientation of the line. This requires a whole set of filter kernels and hence a high computational effort. Therefore, computer-efficient methods are needed to improve the signal-to-noise ratio (SNR).

Guide wire detection is mainly discussed in medical imaging literature under the aspect of enhanced functionality such as position control. As far as image preprocessing is concerned [1], filtering mostly restricts to the application of derivatives of an isotropic, separable kernel. Such filters are not only able to detect lines but also to identify their orientation e.g. by estimating eigenvalues and eigenvectors of the Hessian matrix. However, their applicability for detecting thin lines in very noisy images is limited since the support of the filter kernel is still isotropic.

In image processing literature, filtering with highly orientation-selective filters has been examined in depth in connection with steerable filters [2]. Steerable

**Fig. 1.** Examples of spectra **a, b, c** and filter kernels **d, e, f** for an angular tuning to $\phi_k = \pi/8$. The first two examples (a, b, d, e) are derived using $A(\phi)$ of eq. (1) with $n = 7$ and $n = 15$, last (c, f)for $B(\phi)$ of eq. (2) with $n = 7$.

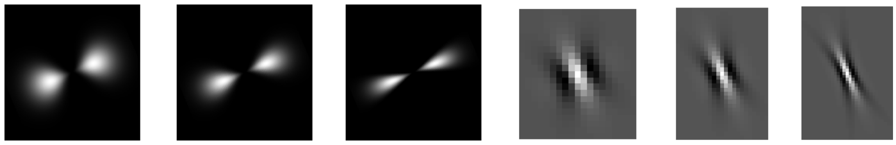

filters allow to calculate a filter response for an arbitrary orientation by linear combination of the responses of a set of basis filters. The angular selectivity of the filters is coupled to the number of basis filters, i.e. increased selectivity implies an increased number of filters and accordingly increased computational effort. So far, the question how to reduce this effort e.g. by appropriate subsampling has not been addressed. Moreover, little is known about how to combine filter responses in order to detect thin straight or curved lines.

In our paper, we present a novel method for detecting thin lines in strongly noise-corrupted images. It consists of the application of a set of orientation-selective anisotropic filters and of the combination of their responses to identify thin continuous lines. To limit the computational effort, a subsampling scheme is used taking into account the orientation of each kernel.

## 2 Method

### 2.1 Filter Design

In a first step, the members of the filter set are constructed in frequency domain. The transfer functions are separable in polar coordinates. A fixed DoG (difference of Gaussians) is used as radial component. The angular component selects a particular angular range. The $n + 1$ members of a filter set are obtained by equidistantly shifting the the angular component. In this paper, we use

$$A_k^n(\phi) = |\cos^n(\phi - \phi_k)| \tag{1}$$

similar to [3] or, with a higher selectivity,

$$B_k^n(\phi) = \begin{cases} \cos^2(\frac{n+1}{2}(\phi - \phi_k)) & \text{if } |\phi - \phi_k + l\pi| < \pi/(n+1), l = 0, 1 \\ 0 & \text{otherwise} \end{cases} , \tag{2}$$

both with $\phi_k = \pi k/(n+1), k = 0, \ldots, n$. Experiments have been carried out with $n = 7$ and $n = 15$ (Fig. 1).

The filter kernels are obtained by approximating the calculated transfer functions in spatial domain. To reduce the filter kernel size, coefficients below a threshold are omitted. In a second step, the coefficients are slightly adjusted to re-establish a zero DC response.

**Table 1.** Subsampling pattern for different filter orientations. Observe that subsampling always takes place in or almost in low pass orientation

| Filter orientation | $]-\pi/8,\pi/8]$ | $]\pi/8,3\pi/8]$ | $]3\pi/8,5\pi/8]$ | $]5\pi/8,7\pi/8]$ |
|---|---|---|---|---|
| subsampling scheme | 1 0 1 0 | 1 1 0 0 | 1 1 1 1 | 1 1 0 0 |
| | 1 0 1 0 | 0 1 1 0 | 0 0 0 0 | 1 0 0 1 |
| | 1 0 1 0 | 0 0 1 1 | 1 1 1 1 | 0 0 1 1 |
| | 1 0 1 0 | 1 0 0 1 | 0 0 0 0 | 0 1 1 0 |

The resulting FIR kernels are thin and elongated and show in one direction a symmetric high pass (second derivative) and in the other a low pass characteristic (Fig. 1). The low pass characteristic allows to sub-sample each of the filter responses without violating the sampling theorem. The number of regular sub-sampling schemes is, however, limited. For a subsampling by a factor of two there are only four possibilities (see Tab. 1).

### 2.2 Line Point Identification

To find points potentially located on a thin line, the filter kernels are applied to the image resulting for each pixel in a vector of responses. These responses now have to be combined to obtain an indication whether a point belongs to a line or not. For bright lines – the situation in X-ray when high radiation is displayed dark – the maximum of all responses turned out to be the best approach. One advantage was that taking the maximum avoided effects due to the negative filter side lobes for points near but not on a line. This scalar maximum filter response provides an indicator for a point being located on a line. This indicator reacts, however, not only on the actual line but also on random structures in noise thus producing worm-like artifacts.

### 2.3 Flood Fill Algorithm

The main difference between random line structures and real lines such as guide wires is that real lines form structures that can be followed over more than a few pixels. Taking only a simple threshold for distinguishing between lines and noise is not sufficient since also real lines are concealed by noise of about the same magnitude at least at some locations. Therefore, the resulting filter response of section 2.2 was subjected to a post-processing. The algorithm starts at the point with maximum filter response which is assumed to be located on the line. Alternatively, all points above a threshold are taken as starting points. The intensity of each point is now set the maximum value for which the point and the starting point can be connected by a path never falling below that value. The idea behind this approach can be seen when thinking of the intensities as a landscape where low means high values in our context. Now starting at the lowest point, the landscape is filled with water.

**Fig. 2.** Processing results. **a** Original image with a SNR of 10 dB. **b** Zoom into a. **c** Processing result for the filter set of eq. (1) with $n = 15$. **d** Result of subsequent modified flood fill algorithm.

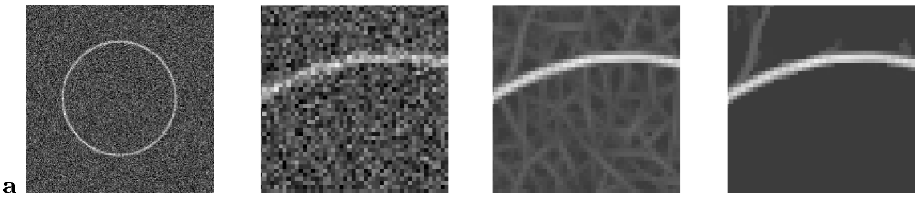


The flood fill algorithm can be further improved by making use of the fact that the curvature of a line is limited. Hence the line orientation will not differ too much between adjacent parts of the same line object. This leads to a *modified* flood fill method in which in contrast to the preceding *isotropic* approach the water flow can only take place if the angular tunings of the individual filter causing the maximum filter response are not too far apart.

## 3 Results

The method has been tested on artificial images and on individual frames from an X-ray fluoroscopy sequence. The artificial images are 1 pixel wide circle shaped lines with Gaussian line profile and a radius of 10–60 pixels. On these images, white Gaussian noise was added ending with a SNR of 10 dB. SNR improvement has been taken as quantitative measure for algorithm performance.

The fluoroscopy sequence shows a cardiovascular examination. A guide wire can be seen moving with the heart beat. Since here no noise-free reference images are available the noise level has been replaced in the SNR calculation by the high frequency image power outside of the guide wire, neglecting the high frequency image signal and the low pass characteristic of X-ray quantum noise.

First, the impact of different filter kernels has been studied. The first step provides a SNR improvement of 11–14 dB (radius = 60 pixel), with higher values for increasing angular resolution. For the same angular resolution, the more selective function (eq. (2)) shows better SNR but stronger response variations along the circle than the one of eq. (1). Similar SNR improvements are obtained for the guide wire images. Fig. 2 shows the original artificial image and the result of this processing step.

Subsampling by a factor of 2 reduces the filter calculation effort by the same factor without any significant change in the results.

Table 2 shows the SNR improvement of the filter response maximum and on the further improved by the isotropic and modified flood filling post processing. As expected, the performance decreases with decreasing radius (increasing curvature). The worm-like artifacts were significantly reduced by the flood-fill post-processing. Moreover, the SNR improvement increased for the modified flood fill algorithm by another 13 dB leading to an overall SNR improvement in case of

**Table 2.** Performance of the algorithm on the artificial images for different circle radii.

| Radius | SNR orig. | SNR maximum filter | SNR flood isotropic | SNR flood modified |
|---|---|---|---|---|
| 60 pixel | 10.39 dB | 23.63 dB | 25.17 dB | 37.18 dB |
| 30 pixel | 10.41 dB | 23.24 dB | 25.12 dB | 26.52 dB |
| 20 pixel | 10.82 dB | 22.71 dB | 24.91 dB | 25.67 dB |
| 10 pixel | 10.43 dB | 19.08 dB | 21.40 dB | 22.26 dB |

**Fig. 3.** Result for the X-ray fluoroscopy image. **a** Original image. **b** result of the maximum filter response. **c** result of the modified flood filling algorithm.

**a**

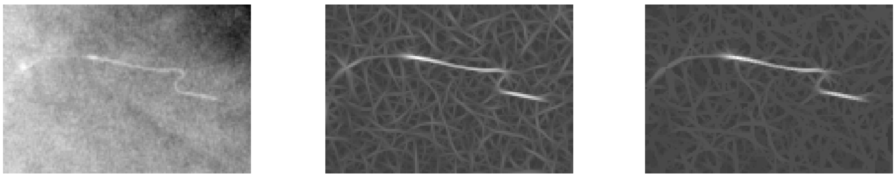

the 60-pixel-radius circle of 27 dB. In case of the X-ray example, an overall SNR improvement of 21 dB was achieved. Visually, the guide wire becomes clearly distinguishable from the surrounding tissue (Fig. 3).

## 4 Discussion

The method described in this paper can be used wherever thin lines are to be discriminated from its surrounding in noisy images. In context of medical imaging, the method can be applied to detect and selectively enhance guide wires in X-ray fluoroscopy images. For a clinical application, the approach has to be integrated into the corresponding image acquisition and processing system to provide benefits for the examining physician. As an example, one may think of selective highlighting of the guide wire. Together with specific algorithms for enhancement of other medically relevant details the method may be used to reduce X-ray dose while keeping the available relevant information in the images unchanged.

## References


1. Baert, Niessen, et al. Guide wire tracking during endovascular interventions. In: Proc. MCCAI 2000; 2000. p. 727–734.
2. Freeman WT, Adelson EH. The Design and Use of Steerable Filters. IEEE Trans PAMI 1991;13(9):891–906.
3. Karasaridis A, Simoncelli E. A filter design technique for Steerable Pyramid image transforms. In: Proc. ICASSP; 1996.